

Article - Human and Animal Health

Preparation of PLGA Nanoparticles Loaded with the Anti-Infective Ctn[15-34] Peptide for Antifungal Application

Ana Paula dos Santos¹

<https://orcid.org/0000-0001-8223-7084>

Roberta Carolina Rangel de Oliveira¹

<https://orcid.org/0000-0002-4193-9300>

Bianca Oliveira Louchard¹

<https://orcid.org/0000-0001-9803-9525>

Antônia Flávia Justino Uchoa²

<https://orcid.org/0000-0003-1717-9839>

Nágila Maria Pontes Silva Ricardo²

<https://orcid.org/0000-0003-1849-5403>

Luzia Kalyne Almeida Moreira Leal¹

<https://orcid.org/0000-0002-3826-2677>

Gandhi Rádis-Baptista³

<https://orcid.org/0000-0001-9210-092X>

Tamara Gonçalves de Araújo^{1*}

<https://orcid.org/0000-0002-1360-479X>

¹Universidade Federal do Ceará, Departamento de Farmácia, Fortaleza, Ceará, Brasil; ²Universidade Federal do Ceará, Departamento de Química Orgânica e Inorgânica, Fortaleza, Ceará, Brasil; ³Universidade Federal do Ceará, Instituto de Ciências do Mar, Fortaleza, Ceará, Brasil;

Editor-in-Chief: Paulo Vitor Farago

Associate Editor: Najeh Maissar Khalil

Received: 19-Oct-2022; Accepted: 18-Jul-2023

*Correspondence: tamara.ufc@gmail.com; Tel.: +55-85-3366 8280 (T.G.A.).

HIGHLIGHTS

- CF-Ctn[15-34] shows excellent encapsulation efficiency (93,3%) in PLGA nanoparticles.
- CF-Ctn[15-34] loaded PLGA nanoparticles have good physicochemical characteristics.
- There is a rapid initial release of the nanoparticles, followed by a sustained release.
- PLGA nanoparticles improves antifungal effect of CF-Ctn[15-34] against *Cryptococcus neoformans*.

Abstract: This article aims to report the preparation and optimized formulation of Ctn[15-34], a designed anti-infective peptide, with poly(lactic acid-co-glycolic acid), PLGA, nanoparticles. Ctn[15-34] is a short peptide derived from crotalidicin, a cathelicidin-related antimicrobial peptide from the venom of the South American rattlesnake (*Crotalus durissus terrificus*), that has arisen as a promising antifungal and microbicide agent. The PLGA nanoparticles were prepared and loaded with carboxyfluorescein (CF)-Ctn[15-34] using the double emulsion/solvent evaporation method. After a preformulation study, which tested different formulation parameters, Poly (vinyl alcohol) 87-89% hydrolyzed and sonication with Sonifier® were chosen to prepare unloaded PLGA nanoparticles by that method, resulting in smaller particle size and Polydispersity Index (PDI) values and higher zeta potential values of nanoparticles. This better condition was used to prepare CF-Ctn[15-34]-loaded PLGA nanoparticles, resulting in homogeneous and spherical nanoparticles, with an average size of 213.2 ± 2.00 nm, PDI of 0.044 ± 0.04 and zeta potential of -16.03 ± 1.20 mV. An excellent encapsulation efficiency was obtained, corresponding to 93.3 ± 0.10 %. The drug-release profile showed a rapid initial release of the peptide, approximately 27 % in the first 24 hours, followed by a sustained

release for at least 16 days. Another relevant aspect in the peptide formulation is that the CF-Ctn[15-34]-loaded nanoparticles potentiated the antifungal effect against the opportunistic pathogenic yeast *Cryptococcus neoformans* compared with the free, in solution Ctn[15-34], in equivalent volume dosage. A preparation method of CF-Ctn[15-34]-loaded PLGA nanoparticles was established and validated, representing a successful approach to deliver CF-Ctn[15-34] for pharmaceutical applications.

Keywords: biocompatible nanoparticle; PLGA; crotalicidin; Ctn[15-34] peptide; anti-infective peptide; antifungal peptide.

INTRODUCTION

The discovery of natural antimicrobial peptides (AMPs) has attracted increasing attention in searching for new therapeutic agents due to their intrinsic properties such as broad-spectrum antimicrobial activity and low tendency to induce microbial resistance [1,2]. In this context, Ctn[15-34] - the C-terminal peptide fragment of crotalicidin (Ctn), a cathelicidin-related AMP from the snake's venom gland of the South American rattlesnake *Crotalus durissus terrificus* emerged as a promising anti-infective peptide [3]. Ctn[15-34] derives from Ctn, and both the full-size Ctn and the Ctn[15-34] fragment have great activity and selectivity against Gram-negative bacteria, pathogenic fungi, and certain types of tumor cells. In addition, the designed Ctn[15-34] reduced the toxicity of the full-length peptide (Ctn) against healthy eukaryotic cells.

Interestingly, the combination of Ctn[15-34] and antifungal drugs restored the minimal inhibitory concentration (MIC) of this class of chemotherapeutics (e.g., amphotericin B) against drug-resistant *Candida* cells. Moreover, in combination with amphotericin B, Ctn[15-34] also reduced the cytotoxicity caused by amphotericin B alone to healthy HK-2 cells and the hemolytic effect on human erythrocytes. These properties reveal an attractive bioactive peptide applicable to pharmaceutical development. In particular, therapeutic and adjuvant alternatives to circumvent the inefficacy of conventional antifungal agents against emergent drug-resistant microbes [3-5]. Besides that, fungal infections represent a serious and continuous threat to human health, causing superficial, cutaneous, subcutaneous, or systemic infections, particularly in immunocompromised or hospitalized individuals [6, 7]. Antifungal drugs like polyenes, azoles, echinocandins, pyrimidine analogs, and allylamines, are used orally, topically, or intravenously to treat infections caused by pathogenic yeasts. However, many of these agents have some disadvantages that limit their therapeutic use due to their toxic side effects, low efficacy, and the emergence of resistant pathogens [8, 9]. In addition, not many antifungal agents have been released in recent years, highlighting the importance of the continuous search for novel compounds and alternatives, such as improving existing formulations, to cope with the current therapeutic demand [2, 10].

Although promising, AMPs generally have a limited therapeutic application due to peptide bioavailability. Using nanotechnology in formulations, the delivery of peptides may represent a practical approach to improving specific pharmacological properties. For example, nanoparticles minimize eventual toxicity caused by peptides to mammalian cells, protect peptides from proteolysis, and unwanted interactions with biological fluids' components and warrant controlled and prolonged peptide drug release [11]. In a recent review, several examples of AMPs and other natural peptides from animal venom advantageously formulated in nanoparticles that turned their use practicable were reported and reemphasized the nanoparticles applicability for venom peptide delivery in the development of therapeutic agents [12].

Among the various types of nanostructures polymeric nanoparticles, especially those based on biocompatibility, poly-lactic-co-glycolic acid (PLGA) is one of the most successful approaches to delivering biologically active peptides [1, 13]. Mainly, this is due to the biodegradability, safety, and biocompatibility of PLGA [14]. In this scenario, considering the impact of fungal infections on human health, the need to expand the arsenal of therapeutics against these opportunistic infectious diseases, the promising antifungal activity exhibited by Ctn[15-34], and the advantages of polymeric nanoparticles for the formulation of bioactive peptides, the study reported the preparation and physicochemical characterization of PLGA nanoparticles loaded with Ctn[15-34] that displayed antifungal activity *in vitro*.

MATERIAL AND METHODS

Materials

Synthetic Ctn[15-34] peptide covalently conjugated with carboxyfluorescein at its C-terminal (CF-Ctn[15-34], MW 2370) obtained with a pure grade over 95% as ascertained by HPLC and MS analysis (China Peptides Co. Ltd., China). Poly-lactic-co-glycolic acid (50:50) (Corbion, Netherlands). Poly(vinyl alcohol) (MW

13,000-23,000, 87-89% hydrolyzed) and Poly(vinyl alcohol) (MW 31,000-50,000, 98-99 % hydrolyzed) (Sigma-Aldrich Ltd., Brazil). Dichloromethane (Sigma-Aldrich Ltd., Brazil). RPMI culture medium (Sigma-Aldrich Ltd., Brazil). Deionized water obtained from the Simplicity® Water Purification System (Merck KGaA, Germany). Amicon® Ultra-15 100 kDa Centrifugal Filter Units (Merck KGaA, Germany). BacTiter-Glo® cell viability reagent (Promega, USA). The clinical strain, drug-resistant *Cryptococcus neoformans* was a gift from Dra. Carolina Sidrim Cavalcante.

Ultra-Turrax® T-25 disperser (IKA, Germany). Sonifier® ultrasonic cell disruptor (Branson Ultrasonics Corp., USA). Zetasizer Nano-S90 zeta potential analyzer (Malvern Instruments, UK). Synergy™ HT multiple detection microplate reader (BioTek, USA). Quanta 450 FEG Scanning Electron Microscope (FEI Company, USA). QT150 ES equipment (Quorum Technologies, USA). DSC 50 Differential Scanning Calorimeter (TA Instruments, USA) DSC cell (Shimadzu, Japan). Q50 TGA Thermogravimetric Analyzer (TA Instruments, EUA).

This study is part of a project registered under the code number A1D1ACF in the platform of the Genetic Heritage Council, Ministry of Environment, Federal Government of Brazil.

Preformulation study of unloaded PGLA nanoparticles

Procedures to prepare unloaded PLGA nanoparticles

Initially, unloaded PLGA nanoparticles (PLGA-NPs) were prepared to ascertain the best formulation conditions. The double emulsion/solvent evaporation (W/O/W) method was adapted from a methodology previously described [15]. Herein, the methodology combined two types of poly (vinyl alcohol) (PVA) and two different types of equipments. Thus, 100 µl of deionized water was added to 5 mL of a 2 % PLGA solution in dichloromethane and emulsified by high-speed homogenization either in a Ultra-Turrax® T-25 instrument (15,000 rpm, for 2 minutes) or by sonication in a Sonifier® instrument (50 % amplitude, for 15 s, in an ice bath). Then, the obtained emulsion in each case was added to 10 mL of an aqueous solution containing 1% PVA 87-89 % hydrolyzed or PVA 98-99 % hydrolyzed and homogenized again in Ultra-Turrax® (24,000 rpm, for 5 min) or Sonifier® (50 % amplitude, 15 s, in an ice bath). The emulsion/solvent mixtures were left stirring overnight to evaporate the solvent, resulting in the suspensions of PLGA-NPs.

Physicochemical evaluation of PLGA-NP

The PLGA-NPs, prepared as aforementioned, were evaluated according to their particle size and polydispersity index (PDI), determined by dynamic light scattering, and had their zeta potential analyzed using a Zetasizer Nano-S90 instrument. The Dynamic light scattering was performed at 25 °C at a fixed angle of 90°. For this analysis, the nanodispersions were diluted in ultrapure water at 1:1000 (v/v) proportion and evaluated in triplicate. Accordingly, conditions for PLGA-NP preparation that resulted in better physicochemical parameters (smaller particle size and PDI values and higher zeta potential values) were further selected to formulate the nanoparticles loaded with the CF-Ctn[15-34] peptides.

Preparation of peptide-loaded nanoparticles (NP-CF-Ctn[15-34])

The methodology used to prepare the NP-CF-Ctn[15-34] considered the best condition founded in preformulation study. Thus, 330 µg of CF-Ctn[15-34] were dissolved in 100 µL of water and added to 5 mL of a 2 % PLGA solution in dichloromethane and emulsified by sonication using a Sonifier® instrument (50 % amplitude, for 15 s, in an ice bath). Then, the obtained emulsion was added to 10 mL of an aqueous solution containing 1% PVA 87-89 % hydrolyzed and homogenized again at same condition. The double emulsion obtained were left stirring overnight to evaporate the solvent, resulting in an aqueous suspension of NP-CF-Ctn[15-34]. These nanoparticles were collected and concentrated using an Amicon® Ultra-15 100 kDa Centrifugal Filter Unit. The ultrafiltrate containing free peptide, which was not loaded in nanoparticles, was quantified by fluorescence. Then, the encapsulation efficiency was calculated, as described in the following section.

Encapsulation efficiency

The peptide incorporated in the nanoparticles was indirectly determined by quantifying the fluorescence of the free peptide that remained in the filtrate previously separated by ultrafiltration. Thus, 50 µl of the filtrate obtained was analyzed with a Synergy™ HT multiple detection microplate reader, with maximum excitation and emission wavelength of 485 nm and 525 nm, respectively. A standard concentration curve for in-solution free fluorescent peptide (CF-Ctn[15-34]) was obtained with a serial dilution of peptide in deionized water,

ranging from 0.78 μM (2.12 $\mu\text{g/mL}$) to 12.5 μM (33.75 $\mu\text{g/mL}$). Subsequently, the encapsulation efficiency was determined by the equation $[(IP - FP)/IP] \times 100$, where IP corresponds to the initial concentration of peptide added to the formulation and FP is the concentration of the free peptide not incorporated into the nanoparticles after the production process.

Loading capacity

The loading capacity (LC) is represented as a mass drug ratio in the nanoparticles to the mass of the recovered nanoparticles it was determined by the equation $[LC = \text{MED}/\text{MR}] \times 100$ where LC corresponds to loading capacity, MED is the mass encapsulated drug (CF-Ctn), MR is the mass recovered of nanoparticles.

Physicochemical evaluation and time-dependent stability of NP-CF-Ctn[15-34]

The analysis of particle size, PDI, and zeta potential was performed for NP-CF-Ctn[15-34] to verify the physicochemical conditions of the system and its stability. The tests were performed at time zero, i.e., just after the preparation of the nanoparticles, and after 30 and 60 days of loaded-nanoparticles storage in aqueous suspension at 4 °C.

Morphological analysis

To observe the morphology, the nanoparticles in the form of a solution were dispersed on a 1 cm^2 glass slide with carbon tape, coated with silver and examined with a magnification of 50000 by Scanning Electron Microscopy (SEM) using a Quanta 450 FEG equipment at a voltage of 30 kV under vacuum by sputtering using a QT150 ES apparatus.

Differential Scanning Calorimetry (DSC)

The physical state analysis of the peptide inside nanoparticles was evaluated using a DSC 50 instrument. The curves were obtained in a DSC cell using an aluminum hermetic pan with approximately 5 mg of samples under a dynamic air atmosphere (40 mL/min) and a heating rate of 10 °C/min in the temperature range from 25 to 600 °C.

Thermogravimetric Analysis (TGA)

The thermal stability of the NP-CF-Ctn[15-34] was conducted using a Q50 TGA instrument. TGA curves were obtained in the temperature range from 30 to 800 °C, using aluminum crucibles with about 2 mg of samples, under dynamic air atmosphere (40 mL/min) and heating rate of 10 °C/min.

In vitro release profile

The release profile of the peptide incorporated in PLGA nanoparticles was determined by *in vitro* analysis using a methodology previously described [15]. Thus, 30 mg of lyophilized NP-CF-Ctn[15-34] were dispersed in 3 mL of phosphate-saline buffer (PBS) – pH 7,4 – and kept under stirring at room temperature for 16 days. After 1 hour and within a time frame of 1 to 16 days of testing, the supernatant (1 mL) was collected through ultrafiltration, and the same volume of PBS was added to the release medium. The release profile was performed in sink condition. A control of free peptide was included in the study. The amount of CF-Ctn[15-34] released at determined times, present in the filtrates, was determined by fluorescence and reported as a cumulative percentage of the peptide released as a function of time.

Antifungal activity of free and encapsulated Ctn[15-34] peptide

The antifungal activity of NP-CF-Ctn[15-34] was evaluated using the luminescent cell viability test with BacTiter-Glo® against a pathogenic, drug-resistant clinical strain of the yeast *Cryptococcus neoformans*, as previously described [4]. In this test, the luminescent signal is proportional to the amount of intracellular ATP, corresponding to the number of viable cells in culture. Thus, the *Cryptococcus neoformans* strains were inoculated on *Sabouraud agar* and incubated at 32 °C for 48 hours to reach the exponential growth phase, ideal for the test. Then, the inoculum suspension was prepared in RPMI culture medium with turbidity adjusted with a UV/VIS spectrophotometer at 550 nm and a cell concentration equivalent to the McFarland standard 0.5 ($\sim 2 \times 10^6$ CFU/mL). Aliquots of yeast suspension (100 μL) were added to 100 μL of CF-Ctn[15-34] solution and NP-CF-Ctn[15-34] suspension separately in microtubes, reaching final concentrations of 5 μM (13.5 $\mu\text{g/mL}$), which is half the MIC (i.e., 10 μM). After incubation (48 h, 30 °C), 50 μL of each of these treatments were transferred, in triplicate, to wells of 96-well microtiter plates. Then, 50 μL of the BacTiter-

Glo® reagent was added to each well to assess fungal viability. The plates were incubated again for 15 minutes at room temperature under gentle agitation, and the luminescence was measured with a Synergy™ HT multiple detection microplate reader. The effect of unloaded nanoparticles on the *Cryptococcus neoformans* growth was also evaluated as control and yeast inoculum not exposed to peptide alone nor to loaded-nanoparticles. The tests were performed in triplicate and expressed as average relative viability (%), with the untreated yeast corresponding to 100 % viability.

Data processing and analysis

All experiments were performed in triplicate, and the results were expressed as mean \pm standard deviation. Analysis of variance (ANOVA) used the F test, and a Tukey's test compared the averages. Differences between groups were significant whether $P < 0.05$.

RESULTS

Physicochemical characterization of unloaded PLGA-NP

Four types of PLGA-NPs were prepared by combining two types of PVAs and two types of equipments, by which particle size, PDI, and zeta potential were determined (Figure 1).

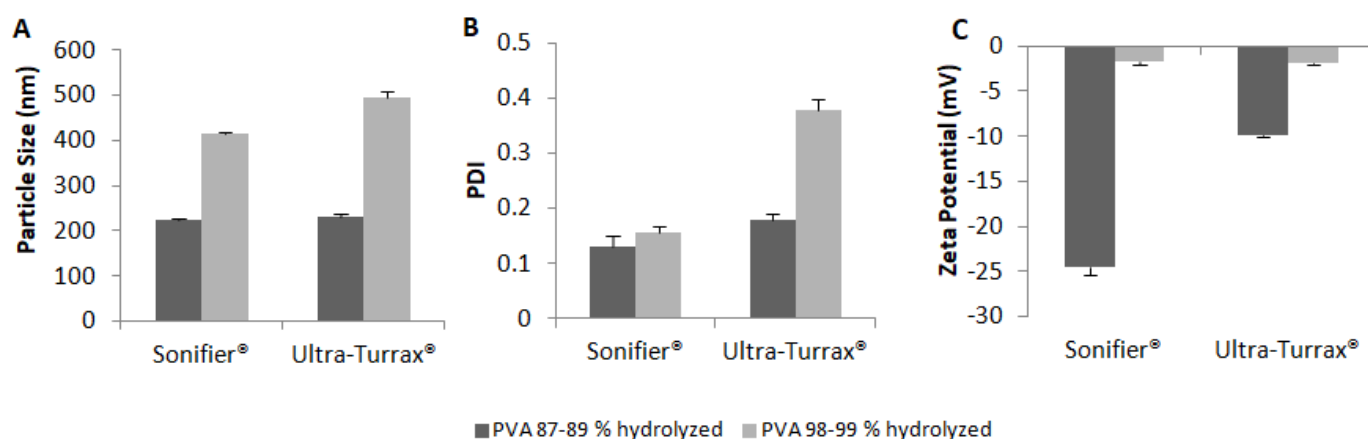


Figure 1. Particle size (A), PDI (B) and zeta potential (C) of PLGA-NP resulting from the combination of two devices (Sonifier® and Ultra-Turrax®) and two types of PVA with different percentages of hydrolysis (87-89 % and 98-99 %) (mean \pm SD, n = 3) $P < 0.05$.

The particle size distribution indicated that less hydrolyzed PVA (87-89%) produced significantly smaller particles (223.4 ± 2.52 and 231.1 ± 6.75 nm) compared to the other type of PVA (416.1 ± 1.42 and 496.4 ± 13.67 nm), regardless of the equipment used. In contrast, more hydrolyzed PVA (98-99%) resulted in larger particles using dispersion with Ultra-Turrax®. The nanoparticles formulated with sonication using Sonifier® showed lower PDI values (0.130 ± 0.02 and 0.157 ± 0.01), regardless of the type of PVA used. Using dispersion with Ultra-Turrax®, higher PDI values were observed (0.180 ± 0.01 and 0.377 ± 0.02), mainly associated with the more hydrolyzed PVA (Figure 1B). As for the zeta potential (Figure 1C), the nanoparticles formulated with less hydrolyzed PVA showed higher absolute values of the zeta potential (more negative values), especially when formulated with sonication in Sonifier® (-24.57 ± 0.74 and -9.84 ± 0.31 mV), in comparison with those formulated with another type of PVA (-1.64 ± 0.40 and -1.95 ± 0.16 mV). In addition, the nanoparticle preparation with Ultra-Turrax® using the less hydrolyzed PVA caused the formation and overflow of a large amount of foam, with loss of components. Given these results, less hydrolyzed PVA (87-89 %), as a stabilizer, and sonication with Sonifier® were selected to formulate the NP-CF-Ctn[15-34].

Peptide-loaded nanoparticles

Physicochemical evaluation and time-dependent stability of NP-CF-Ctn[15-34]

The size of prepared NP-CF-Ctn[15-34] fitted into a nanometric range, with an average particle size of 213.2 ± 2.00 nm. The PDI and zeta potential values obtained were 0.044 ± 0.04 and -16.03 ± 1.20 mV, respectively. The peptide nanosystem stored in an aqueous suspension at 4° C remained stable, from a physicochemical point of view, for 30 days, with minimal variations in the overall composition up to 60 days.

Minimal variations included a slight increase in the average particle size and a slight reduction in absolute values of zeta potential with an extended time of 60 days of storage. There was no statistical difference in these characteristics for the PDI values at different times of analysis (Figure 2).

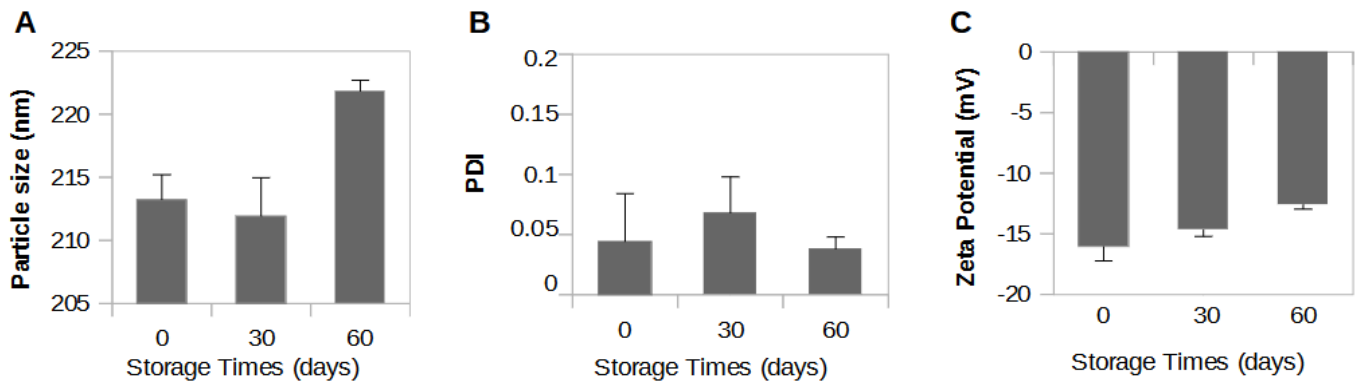


Figure 2. Particle size (A), PDI (B) and zeta potential (C) of NP-CF-Ctn[15-34] evaluated at different storage times in aqueous suspension at 4 °C. (mean ± SD, n = 3) P <0.05.

Morphological analysis of NP-CF-Ctn[15-34]

The morphological analysis by SEM showed essentially spherical nanoparticles and confirmed the average nanoscale size (Figure 3).

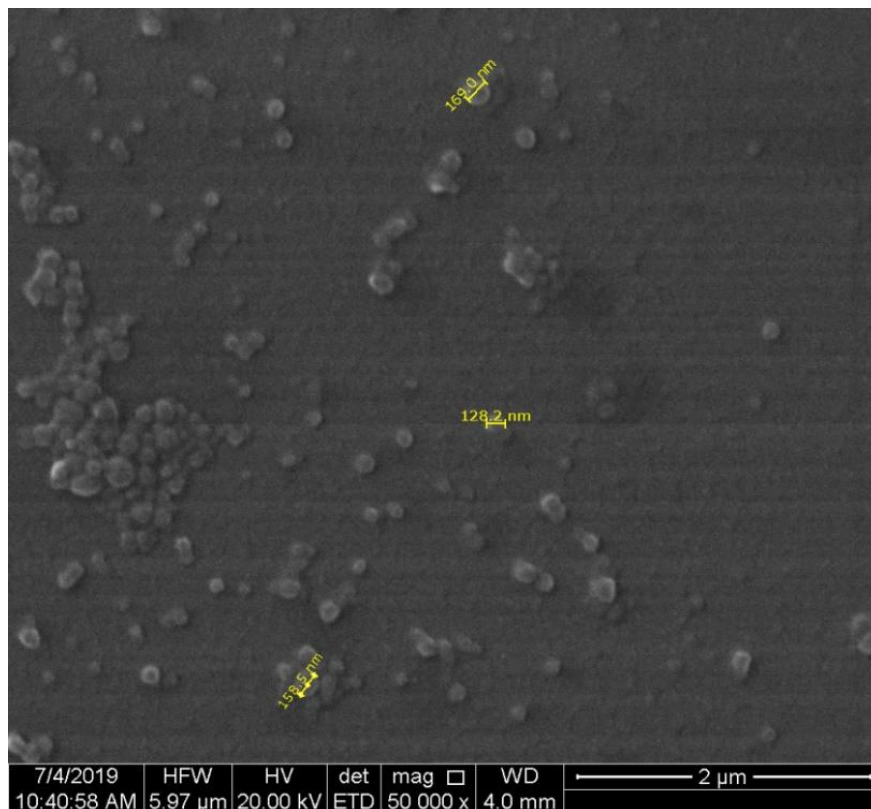


Figure 3. Scanning electron microscope image of the NP-CF-Ctn[15-34].

Differential Scanning Calorimetry (DSC)

The thermogram curves represent the thermal properties of the nanoparticle components and the state of the CF-Ctn[15-34] after the encapsulation process (Figure 4).

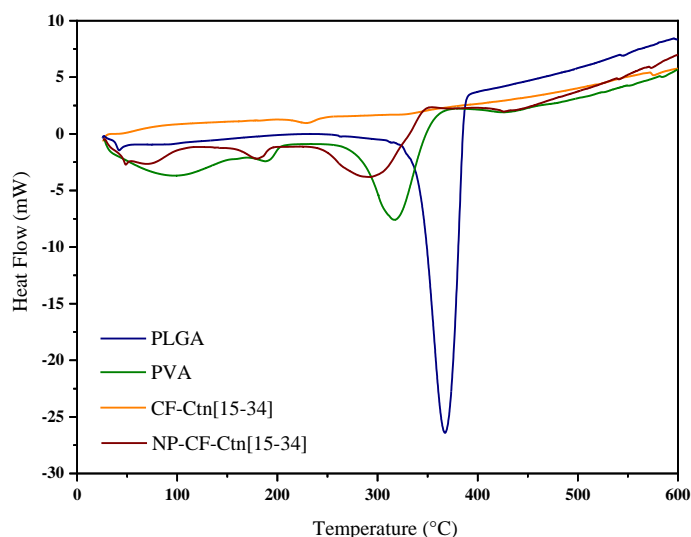


Figure 4. DSC curves of the PLGA nanoparticles: CF-Ctn[15-34] peptide (orange), PLGA (navy), PVA (87-89 % hydrolysed) (olive) and NP-CF-Ctn[15-34] (wine).

The CF-Ctn[15-34] peptide showed a glass transition temperature (T_g) of 42.33 °C and an endothermic peak of 229.3 °C. PLGA presented a T_g of 42.27 °C and an endothermic peak at 366.8 °C, while PVA exhibited three endothermic events at 95.28, 188.3, and 315.6 °C. It is possible to observe that the same thermal events observed for the isolated PVA and PLGA are also on the NP-CF-Ctn[15-34] curve. On the other hand, crystallinity events related to the entrapped peptide was not detected since the TGA curve did not show an endothermic peak related to this effect (see below).

Thermogravimetric Analysis (TGA)

The TGA was used to evaluate the thermal stability of NP-CF-Ctn[15-34] in a wide range of temperatures (from 0 °C to 150 °C), compared to polymer (Figure 5). The decomposition process took place in two stages, the first at 282.19 °C (73.48 %) and the second at 434.39 °C (22.44 %), associated with exothermic events.

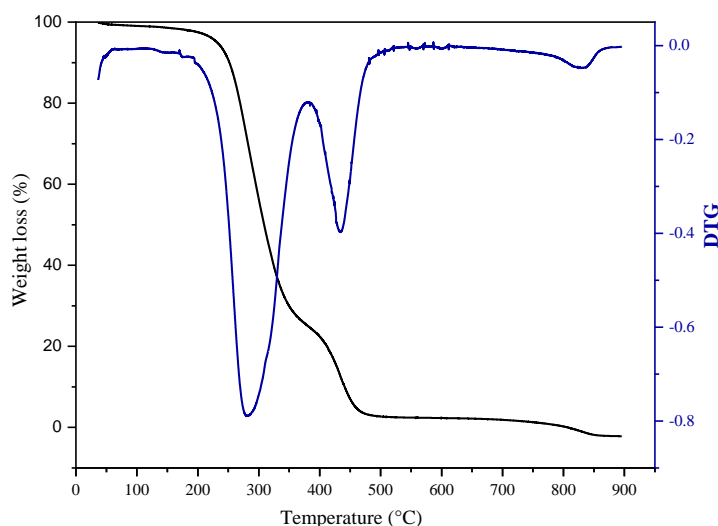


Figure 5. TGA curve of NP-CF-Ctn[15-34].

Encapsulation efficiency

According to the fluorescence standard curve for CF-Ctn[15-34], the equation parameters were defined from $y = 5581.4x - 4033$, where y is the measured fluorescence and x is the concentration (μM) of CF-Ctn[15-34] in solution. The linear correlation coefficient (R^2) obtained was 0.9987. The concentration of peptide that remained in the solution, not incorporated in the nanoparticles, was only 0.8154 μM (2.2 $\mu\text{g/mL}$), based on the standard curve. Considering the initial concentration of 33 $\mu\text{g/mL}$ of CF-Ctn[15-34] throughout the nanosystem preparation, the encapsulation efficiency reached $93.3 \pm 0.10\%$.

Loading capacity

The theoretical total amount that was predicted in the development of the formulation was that in each 1 mL of nanoparticle solution it would contain 33 ug of the CF-Ctn[15-34] drug, and the actual amount experimentally determined by fluorescence measurement was 30.8 ug/mL of CF-Ctn[15-34] in the nanoparticle solution. The calculation of loading capacity showed a value of 0.1537wt%.

In vitro release profile of NP-CF-Ctn[15-34]

The release profile of CF-Ctn[15-34] from nanoparticles *in vitro* was measured for 16 days (Figure 6). Approximately 27 % of the peptide was detected in the supernatant along the first day of testing. Of which 14 % was released in the first hour, indicating a rapid onset of peptide release. After that, a sustained release of CF-Ctn[15-34] peptide added up to about 80 % release by the last day of testing. Free peptide was completely in solution in the first hour.

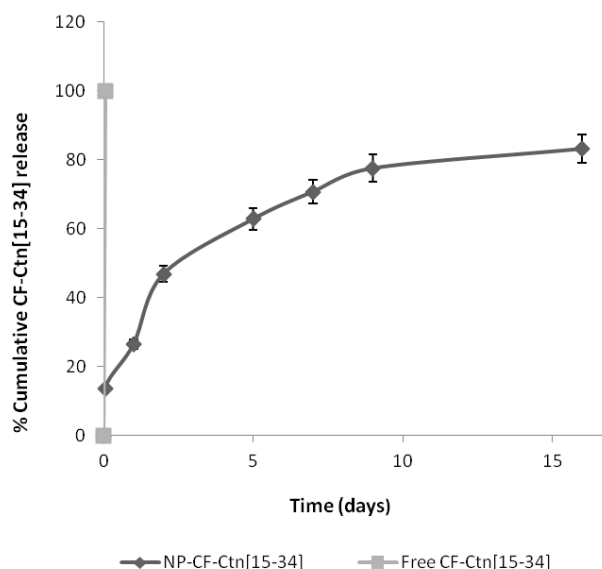


Figure 6. Cumulative *in vitro* release of CF-Ctn[15-34] from PLGA nanoparticles and free CF-Ctn[15-34] in PBS medium (pH 7.4).

Antifungal activity of the free and encapsulated peptide

NP-CF-Ctn[15-34] markedly reduced pathogenic fungal growth up to 73 %, resulting in fungal viability to only 27.0 ± 4.68 % compared to the untreated group (negative control). The treatment with CF-Ctn[15-34] in solution resulted, in contrast, in fungal viability of 66.5 ± 7.81 % (at 5µM, the MIC), with a reduction in *Cryptococcus* cell viability of approximately 35% (Figure 7). Instead of showing antifungal activity, the unloaded nanoparticles (PLGA-NP) did the opposite and promoted a slight fungal growth.

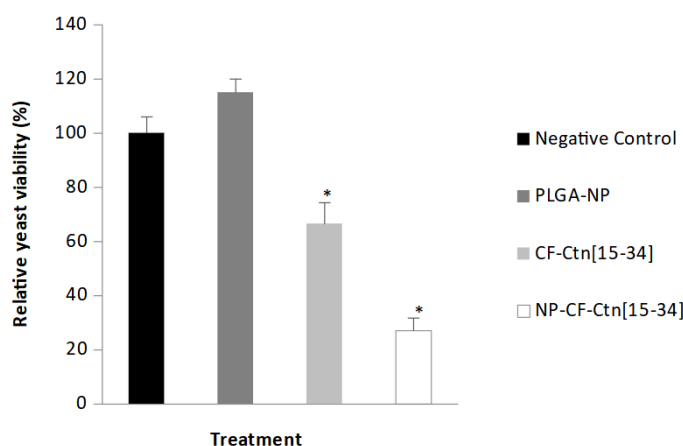


Figure 7. Antifungal activity of CF-Ctn[15-34] and NP-CF-Ctn[15-34] against *Cryptococcus neoformans* (mean ± SD, n = 3) * P <0.05. Statistical significance compared to negative control.

DISCUSSION

The double emulsion/solvent evaporation process is considered an optimal and practical method for encapsulating peptides [16]. In this study, its use resulted in nanoparticles successfully loaded with CF-Ctn[15-34]. Less hydrolyzed PVA resulted in smaller nanoparticles. Consequently, it was more efficient to prepare polymeric nanoparticles, as noticed previously by others [17]. The smaller-sized particles usually display a better *in vitro* and *in vivo* performance, as exemplified by enhanced cellular uptake. Particle sizes in the 200 nm range are adequate for this purpose [18, 19].

In contrast, more hydrolyzed PVA resulted in larger nanoparticles. The numerous hydroxyls present may form intra- and intermolecular hydrogen bonds [20]. The increase in the hydrolysis level of PVA also affects several physical characteristics: it reduces the solubility and increases water resistance, adhesion to hydrophilic surfaces, viscosity, and tensile strength. This increase in viscous resistance seems to be responsible for the absorption of the homogenization energy, reducing shear forces, resulting in larger droplets, as previously noted [21]. In addition, the negative effect of increasing the percentage of hydrolysis on particle size was more expressive when using Ultra-turrax® and compared with Sonifier®. Dispersions in aqueous systems caused by ultrasound rely on cavitation [22], while high-speed homogenization increases the shear force overcoming internal forces acting on the particles [23]. According to the equipment used for particle preparation, these differences influence the particle nanostructures and the particle PDI. The PDI values obtained with Sonifier® were below the limit of 0.2, representing a homogeneous nanoparticle size distribution [24]. Although higher, PDI values of NPs prepared with Ultra-Turrax® and the less hydrolyzed PVA were also within the expected limit. Nevertheless, using the Ultra-Turrax® with the more hydrolyzed PVA, the PDI values of NPs indicated a heterogeneous dispersion and, therefore, less acceptable. Concerning the zeta potential, the formulations obtained with more hydrolyzed PVA again displayed inferior characteristics, with zeta potential values close to zero. The negative charge of the zeta potential results from the dissociation of acid groups originating from PLGA on the surface of the particles [25]. The more distant from zero the zeta potential values are, the better is the electrostatic stabilization of the system, with less possibility of aggregation due to the greater repulsion of the charges between the particles [26]. Absolute values of 20 mV or less can only provide short-term stability; however, PVAs of higher molecular mass stabilize the particles, resulting in acceptable zeta potential values [27].

Then, particles loaded with the anti-infective peptide were formulated using the best-selected experimental conditions: the less hydrolyzed PVA and sonication with Sonifier®. The morphological analysis showed essentially spherical nanoparticles formed (Figure 3). The NP-CF-Ctn[15-34] size was in the nanometric range from 200 ± 3.69 nm to 304.5 ± 10.0 nm, using double emulsion/solvent evaporation methods [15, 28]. For NP-CF-Ctn[15-34], the low PDI values indicate a homogeneity in particles' size. There was a reduction in absolute values of the zeta potential from -24.57 ± 0.74 mV to -16.03 ± 1.20 mV, in contrast to unloaded nanoparticles. In agreement with other preparation, similar values (-15.53 ± 0.71 mV) [27] and higher values (-21.93 ± 2.93 and -27.2 ± 1.9 mV) were found for PLGA nanoparticles loaded with peptides [29, 30]. The reduction in absolute values of the zeta potential may be related to the physical and chemical characteristics of CF-Ctn[15-34], which is not only carried inside the particles but also might contribute to the overall nanostructure.

The nanoparticles maintained their physicochemical stability in suspension for over 30 days, possibly due to a combination of electrostatic and steric stabilization, showing minimal variations even when the period of particle storage extended as long as 60 days (Figure 2). The DSC analysis showed that the nanoparticle production method did not affect the structure of the PVA and PLGA (Figure 4) in loaded nanoparticles. The same thermal events were similar for the isolated PVA, PLGA, and NP-CF-Ctn[15-34]. On the other hand, particle-entrapped peptides did not show any crystallinity. Such data suggested that the active principle (peptide) incorporated in the nanoparticles may be in amorphous form or a non-crystalline phase dispersed in the polymeric matrix, as documented by other authors for distinct peptides [31,32]. The TGA indicated that the in-solution controlled decomposition of NP-CF-Ctn[15-34] occurred in 2-stages (Figure 5). In this sense, higher levels of degradation occur because of the submicrometric size and the larger surface area of the nanoparticles, which makes smaller nanoparticles prone to greater exposure and, consequently, more significant thermal degradation [33].

As high as 93.3 %, high encapsulation efficiency was reached using the optimized procedure and the selected experimental conditions for NP-CF-Ctn[15-34] preparation. Encapsulation efficiency is essential to obtain economically formulated nanoparticles for further therapeutic application [34]. High efficiency of encapsulation of other peptides incorporated in PLGA nanoparticles using the double emulsion/solvent evaporation method, supporting the present selected methodological choice [15, 18, 28, 35]. The calculation of loading capacity showed a value of 0.1537wt%. This value represents a low load capacity, but this low

capacity was already expected in the development of the formulation, since the intention was to add a high concentration of polymer to guarantee a high incorporation of the drug in the nano structures. Moreover, the net positive charge of CF-Ctn[15-34], a cationic peptide, appeared to contribute to self-peptide incorporation into particles due to electrostatic interaction with the negatively charged PLGA. Thus, incorporating CF-Ctn[15-34] in PLGA nanoparticles may provide a prolonged release of the peptide, as observed elsewhere for other similar delivery systems [18]. Notably, the rapid initial release of active ingredients, like peptides, is expected to occur if the drugs are loosely bound or adsorbed to the surface of nanoparticles [13].

In fact, *in vitro* analysis of NP-CF-Ctn[15-34] showed an improved antifungal effect compared to free, in-solution CF-Ctn[15-34], causing a superior 75% reduction in the cell viability of the pathogenic, clinically-relevant yeast *Cryptococcus neoformans* cells compared to free CF-Ctn[15-34] (~35 % reduction). Moreover, unloaded PLGA nanoparticles appeared to promote the growth of *Cryptococcus neoformans* cells, probably, by serving as a carbon source or a solid surface for cell adhesion (Figure 7). PLGA nanoparticles loaded with conventional antifungal drugs, such as amphotericin B [36], and nanoparticles loaded with natural compounds, such as the juglone [37], also display similar effects. These formulations have shown enhanced antifungal activity *in vitro* compared with active ingredients in solution. Thus far, nanotechnological tools in pharmaceutical science and drug delivery are indispensable for formulations of both novel and conventional antifungal substances individually or in drug combination [38]. In the present study, *Cryptococcus neoformans* was chosen as the target microbial cell to test the peptide-loaded nanoparticles because this pathogenic yeast is an opportunistic infectious agent that together with *Cryptococcus gattii*, causes Cryptococcosis, a lethal fungal disease, particularly for immunocompromised patients with acquired immunodeficiency syndrome (AIDS) [39]. The strain of *Cryptococcus neoformans* used herein is a clinical isolate from cerebrospinal fluid that is resistant to amphotericin B (MIC = >16 µg/mL or >16 µM), and fluconazole (MIC = >200 µg/mL or >64 µM), but sensitive to the Ctn[15-34] peptide (MIC = 5 µg/mL or 11.85 µM) [5].

The mechanism of CF-Ctn[15-34] release from nanoparticles deserves further investigation. The unconjugated unloaded Ctn[15-34] is a peptide that kills Gram-negative bacteria and pathogenic yeasts (*Candida* and *Cryptococcus*). First, it disrupts the plasma membrane, then interacts with the microbial DNA, and induces the death of the cell by early apoptosis and later necrosis processes [5, 40, 41]. It was hypothesized that the negative charge of the PLGA nanoparticles promotes their interaction with the positively charged polysaccharides of the *Cryptococcus neoformans* capsule. This electrostatic interaction would facilitate the accumulation on the cell surface and, possibly the entry into the cells, slowly releasing the peptide to exert their effect at the membrane by pore formation. Particles with a size close to 200 nm were captured and internalized by fungal cells [37]. Moreover, the increased number of molecules per nanoparticle volume makes peptides much more available to target cells, contributing to this enhanced antifungal effect, as seen here for the NP-CF-Ctn[15-34].

CONCLUSION

Finding more potent, less harmful, and affordable treatment options against severe, drug-resistant fungal disease is demanding in clinical sets, so the formulation of drug-loaded PLGA nanoparticles has proven to be a valuable resource. The preparation of drug-loaded nanoparticles is cost-effective for delivering various bioactive agents, including peptides. Herein, the formulation of nanoparticles of PLGA loaded with the peptide Ctn[15-34], a promising anti-infective and antifungal agent, was achieved. The resultant CF-Ctn[15-34]-loaded nanoparticles showed ideal physicochemical characteristics and excellent encapsulation efficiency. Notably, the CF-Ctn[15-34] was efficiently delivered to its target, the opportunistic yeast *Cryptococcus neoformans*, improving the antifungal effect compared to the free, in-solution peptide. These data represent a prospective pharmaceutical strategy to deliver Ctn[15-34] topically or systemically in further *in vivo* studies.

Funding: This research was funded by Ceara Foundation of Support for Scientific and Technological Development (FUNCAP).

Acknowledgments: Authors are grateful for the Ceara Foundation of Support for Scientific and Technological Development (FUNCAP), the Central Analítica-UFC/CT-INFRA/MCTI-SISNANO/CAPES, the National Council for Scientific and Technological Development (CNPq), the Ministry of Science, Technology, and Innovation (MCTI), the Federal Government of Brazil and the Coordination for the Improvement of Higher Education Personnel (CAPES), the Ministry of Education and Culture, the Federal Government of Brazil.

Conflict of interests: The authors declare no conflict of interest.

REFERENCES

1. Almaaytah A, Mohammed GK, Abualhajjaa A, Al-Balas Q. Development of novel ultrashort antimicrobial peptide nanoparticles with potent antimicrobial and antibiofilm activities against multidrug-resistant bacteria. *Drug Des Devel Ther.* 2017 Nov;11:3159-3170. doi: 10.2147/DDDT.S147450.
2. Ciociola T, Giovati L, Conti S, Magliani W, Santinoli C, Polonelli L. Natural and synthetic peptides with antifungal activity. *Future Med Chem.* 2016 Aug;8(12):1413-33. doi: 10.4155/fmc-2016-0035.
3. Falcao CB, Pérez-Peinado C, de la Torre BG, Mayol X, Zamora-Carreras H, Jiménez MÁ, et al. Structural dissection of crotalicidin, a rattlesnake venom cathelicidin, retrieves a fragment with antimicrobial and antitumor activity. *J Med Chem.* 2015 Oct;58(21):8553–63. doi:10.1021/acs.jmedchem.5b01142.
4. Cavalcante CS, Falcão CB, Fontenelle RO, Andreu D, Rádis-Baptista G. Anti-fungal activity of Ctn[15-34], the C-terminal peptide fragment of crotalicidin, a rattlesnake venom gland cathelicidin. *J Antibiot.* 2017 Mar;70(3):231-7. doi: 10.1038/ja.2016.135.
5. De Aguiar FLL, Cavalcante CSDP, Dos Santos Fontenelle RO, Falcão CB, Andreu D, Rádis-Baptista G. The antiproliferative peptide Ctn [15-34] is active against multidrug-resistant yeasts *Candida albicans* and *Cryptococcus neoformans*. *J Appl Microbiol.* 2020 Feb;128(2):414-425. doi: 10.1111/jam.14493.
6. Gupta M, Sharma V, Chauhan NS. Promising novel nanopharmaceuticals for improving topical antifungal drug delivery. In: Grumezescu AM, editor. *Nano- and microscale drug delivery systems: design and fabrication.* Elsevier; 2017. p. 197-228. doi.org/10.1016/B978-0-323-52727-9.00011-X.
7. Sawant B, Khan T. Recent advances in delivery of antifungal agents for therapeutic management of candidiasis. *Biomed Pharmacother.* 2017 Dec;96:1478-1490. doi: 10.1016/j.biopha.2017.11.127.
8. Campoy S, Adrio JL. Antifungals. *Biochem Pharmacol.* 2017 Jun;133:86-96. doi: 10.1016/j.bcp.2016.11.019.
9. Van der Weerden NL, Bleackley MR, Anderson MA. Properties and mechanisms of action of naturally occurring antifungal peptides. *Cell Mol Life Sci.* 2013 Oct;70(19):3545-70. doi: 10.1007/s00018-013-1260-1.
10. Souza AC, Amaral AC. Antifungal therapy for systemic mycosis and the nanobiotechnology era: improving efficacy, biodistribution and toxicity. *Front Microbiol.* 2017 Mar;8:336. doi: 10.3389/fmicb.2017.00336.
11. Sandreschi S, Piras AM, Batoni G, Chiellini F. Perspectives on polymeric nanostructures for the therapeutic application of antimicrobial peptides. *Nanomedicine.* 2016 Jul;11(13):1729-44. doi: 10.2217/nnm-2016-0057.
12. Dos Santos AP, de Araújo TG, Rádis-Baptista G. Nanoparticles Functionalized with Venom-Derived Peptides and Toxins for Pharmaceutical Applications. *Curr Pharm Biotechnol.* 2020;21(2):97-109. doi: 10.2174/1389201020666190621104624.
13. Allahyari M, Mohit E. Peptide/protein vaccine delivery system based on PLGA particles. *Hum Vaccin Immunother.* 2016 Mar;12(3):806-28. doi: 10.1080/21645515.2015.1102804.
14. Vysloužil J, Doležel P, Kejdušová M, Mašková E, Mašek J, Lukáč R, et al. Influence of different formulations and process parameters during the preparation of drug-loaded PLGA microspheres evaluated by multivariate data analysis. *Acta Pharm.* 2014 Dec;64(4):403–17. doi: 10.2478/acph-2014-0032.
15. Chereddy KK, Her CH, Comune M, Moia C, Lopes A, Porporato PE, et al. PLGA nanoparticles loaded with host defense peptide LL37 promote wound healing. *J Control Release.* 2014 Nov;194:138–47. doi:10.1016/j.jconrel.2014.08.016.
16. Iqbal M, Zafar N, Fessi H, Elaissari A. Double emulsion solvent evaporation techniques used for drug encapsulation. *Int J Pharm.* 2015 Dec;496(2):173-90. doi: 10.1016/j.ijpharm.2015.10.057.
17. Yang M, Lai SK, Yu T, Wang YY, Happe C, Zhong W, et al. Nanoparticle penetration of human cervicovaginal mucus: the effect of polyvinyl alcohol. *J Control Release.* 2014 Oct;192:202-8. doi: 10.1016/j.jconrel.2014.07.045.
18. Derman S, Mustafaeva ZA, Abamor ES, Bagirova M, Allahverdiyev A. Preparation, characterization and immunological evaluation: canine parvovirus synthetic peptide loaded PLGA nanoparticles. *J Biomed Sci.* 2015 Oct;22:89. doi: 10.1186/s12929-015-0195-2.
19. Zhao H, Lin ZY, Yildirimer L, Dhinakar A, Zhao X, Wu J. Polymer-based nanoparticles for protein delivery: design, strategies and applications. *J Mater Chem B.* 2016 Jun;4(23):4060-71. doi: 10.1039/c6tb00308g.
20. Aranha IB, Lucas EF. [Chemical modification of poly(vinyl alcohol): evaluation of hydrophilic/lipophilic balance]. *Polímeros.* 2001;11(4):174–81. doi: 10.1590/S0104-14282001000400007
21. Crucho CIC, Barros MT. Polymeric nanoparticles: a study on the preparation variables and characterization methods. *Mater Sci Eng C Mater Biol Appl.* 2017 Nov;80:771-784. doi: 10.1016/j.msec.2017.06.004.
22. Svilenov H, Tzachev C. Solid lipid nanoparticles – a promising drug delivery system. In: Seifalian A, de Mel A, Kalaskar DM, editors. *Nanomedicine.* Manchester: One Central Press Ltd; 2014. p.187–237.
23. Arasoğlu T, Derman S, Mansuroğlu B, Uzunoğlu D, Koçyiğit B, Gümüş B, et al. Preparation, characterization, and enhanced antimicrobial activity: quercetin-loaded PLGA nanoparticles against foodborne pathogens. *Turk J Biol.* 2017;41(1):127–40. doi:10.3906/biy-1604-80.
24. Danaei M, Dehghankhold M, Ataei S, Hasanzadeh Davarani F, Javanmard R, Dokhani A, et al. Impact of particle size and polydispersity index on the clinical applications of lipidic nanocarrier systems. *Pharmaceutics.* 2018 May;10(2):57. doi: 10.3390/pharmaceutics10020057.
25. Malvern Instruments Limited. Zeta potential - an introduction in 30 minutes [Internet]. [place unknown: publisher unknown]; [updated 2020; cited 2022 Set 24]. Available from: <https://www.malvernpanalytical.com/en/learn/knowledge-center/technical-notes/TN101104ZetaPotentialIntroduction>.

26. Lin PC, Lin S, Wang PC, Sridhar R. Techniques for physicochemical characterization of nanomaterials. *Biotechnol Adv.* 2014 Jul-Aug;32(4):711-26. doi: 10.1016/j.biotechadv.2013.11.006.
27. Honary S, Zahir F. Effect of zeta potential on the properties of nano-drug delivery systems - a review (Part 2). *Trop J Pharm Res.* 2013 May;12(2). doi:10.4314/tjpr.v12i2.20.
28. Han HD, Byeon Y, Kang TH, Jung ID, Lee JW, Shin BC, et al. Toll-like receptor 3-induced immune response by poly(d,l-lactide-co-glycolide) nanoparticles for dendritic cell-based cancer immunotherapy. *Int J Nanomedicine.* 2016 Nov;11:5729-5742. doi: 10.2147/IJN.S109001.
29. Hiremath J, Kang KI, Xia M, Elaish M, Binjawadagi B, Ouyang K, et al. Entrapment of H1N1 influenza virus derived conserved peptides in PLGA nanoparticles enhances t cell response and vaccine efficacy in pigs. *PLoS One.* 2016 Apr;11(4):e0151922. doi: 10.1371/journal.pone.0151922.
30. Song C, Noh YW, Lim YT. Polymer nanoparticles for cross-presentation of exogenous antigens and enhanced cytotoxic T-lymphocyte immune response. *Int J Nanomedicine.* 2016 Aug;11:3753-64. doi: 10.2147/IJN.S110796.
31. Pirooznia N, Hasannia S, Lotfi AS, Ghanei M. Encapsulation of alpha-1 antitrypsin in PLGA nanoparticles: in vitro characterization as an effective aerosol formulation in pulmonary diseases. *J Nanobiotechnology.* 2012 May;10:20. doi: 10.1186/1477-3155-10-20.
32. Sun SB, Liu P, Shao FM, Miao QL. Formulation and evaluation of PLGA nanoparticles loaded capecitabine for prostate cancer. *Int J Clin Exp Med.* 2015 Oct;8(10):19670-81. doi: 10.1590/S1516-93322006000400007.
33. Mainardes RM, Gremião MPD, Evangelista RC. Thermoanalytical study of praziquantel-loaded PLGA nanoparticles. *Rev Bras Cienc Farm.* 2006 Dec;42(4):523-30.
34. Amini Y, Amel Jamehdar S, Sadri K, Zare S, Musavi D, Tafaghodi M. Different methods to determine the encapsulation efficiency of protein in PLGA nanoparticles. *Biomed Mater Eng.* 2017;28(6):613-620. doi: 10.3233/BME-171705.
35. Ma W, Chen M, Kaushal S, McElroy M, Zhang Y, Ozkan C, et al. PLGA nanoparticle-mediated delivery of tumor antigenic peptides elicits effective immune responses. *Int J Nanomedicine.* 2012;7:1475-87. doi: 10.2147/IJN.S29506.
36. Asghari H, Nanekarani S. Antifungal activity of amphotericin b-loaded nanoparticles. *J Adv Agric Technol.* 2016; 3(1):26-29. doi:10.18178/joaat.3.1.26-29.
37. Arasoglu T, Mansuroglu B, Derman S, Gumus B, Kocyigit B, Acar T, et al. Enhancement of antifungal activity of juglone (5-hydroxy-1,4-naphthoquinone) using a poly(d,l-lactic-co-glycolic acid) (PLGA) nanoparticle system. *J Agric Food Chem.* 2016 Sep;64(38):7087-94. doi: 10.1021/acs.jafc.6b03309.
38. Scorzoni L, Sangalli-Leite F, de Lacorte Singulani J, de Paula E Silva AC, Costa-Orlandi CB, Fusco-Almeida AM, et al. Searching new antifungals: the use of *in vitro* and *in vivo* methods for evaluation of natural compounds. *J Microbiol Methods.* 2016 Apr;123:68-78. doi: 10.1016/j.mimet.2016.02.005.
39. Kwon-Chung KJ, Bennett JE, Wickes BL, Meyer W, Cuomo CA, Wollenburg KR, et al. The case for adopting the "species complex" nomenclature for the etiologic agents of cryptococcosis. *mSphere.* 2017 Jan;2(1):e00357-16. doi: 10.1128/mSphere.00357-16.
40. Cavalcante CSP, de Aguiar FLL, Fontenelle ROS, de Menezes RRPB, Martins AMC, Falcão CB, et al. Insights into the candidacidal mechanism of Ctn[15-34] - a carboxyl-terminal, crotalidicin-derived peptide related to cathelicidins. *J Med Microbiol.* 2018 Jan;67(1):129-138. doi: 10.1099/jmm.0.000652.
41. Pérez-Peinado C, Dias SA, Domingues MM, Benfield AH, Freire JM, Rádis-Baptista G, et al. Mechanisms of bacterial membrane permeabilization by crotalidicin (Ctn) and its fragment Ctn(15-34), antimicrobial peptides from rattlesnake venom. *J Biol Chem.* 2018 Feb;293(5):1536-1549. doi: 10.1074/jbc.RA117.000125



© 2023 by the authors. Submitted for possible open access publication under the terms and conditions of the Creative Commons Attribution (CC BY NC) license (<https://creativecommons.org/licenses/by-nc/4.0/>).